Phase Instability in Semiconductor Lasers

L. Gil* and G. L. Lippi
Université de Nice-Sophia Antipolis, CNRS, Institut Non-Linéaire de Nice, UMR 7335, F-06560, France
(Received 10 February 2014; published 21 November 2014)

For many years, the apparent absence of a phase instability has characterized lasers as *peculiar* nonlinear oscillators. We show that this unusual feature is solely due to the approximations used in writing the standard models. A new, careful derivation of the fundamental equations, based on codimension 2 bifurcation theory, shows the possible existence of dynamical regimes displaying either a pure phase instability, or mixed phase-amplitude turbulence. A comparison to existing experimental results convincingly shows that the Benjamin-Feir instability, common to all nonlinear wave problems, is a *fundamental*, satisfactory interpretation for their deterministic multimode dynamics.

DOI: 10.1103/PhysRevLett.113.213902 PACS numbers: 42.55.Px, 42.55.Ah, 42.60.Mi

The phase instability is a generic driving mechanism for spatiotemporal complexity, first discovered in fluid dynamics a few decades ago [1]. It is a universal mechanism which is to be expected whenever waves are present, irrespective of the physics domain under study. In nonlinear optics this instability is better known under the name of *modulational instability* and appears mainly in the description of pulse formation in optical fibers [2].

Quite surprisingly, the phase instability has never been invoked in modeling the complex spatiotemporal behavior observed in semiconductor lasers. Indeed, up until recently lasers had been considered by the nonlinear physics community as somewhat anomalous (nonlinear) oscillators, given their apparent constant emission frequency for all field strength values [3] and, notably, the absence of a phase-unstable regime of operation.

Complex dynamics has been known, although not necessarily recognized as such, since the early observations of laser emission. In particular, the light output by semiconductor lasers has been recognized as being particulary *noisy* and extensive studies were conducted mainly in the 1980s. Given the multimode nature of semiconductor lasers (i.e., emission on different optical frequencies), two main, noise-driven regimes of operations were identified, characterized by irregular longitudinal mode switching [4–6]: (i) mode partition, where the total laser power fluctuates among several coexisting longitudinal modes [7,8], and (ii) mode hopping, where only one mode at a time is emitting [8,9].

When the issue of the multimode dynamics appeared to be settled, an *unusual* multimode regime was experimentally reported [10,11] in "short wavelength" ($\lambda \approx 850$ nm) multiple-quantum-well semiconductor lasers. Its dynamics was characterized by a regular modal alternating with periodic oscillation of the optical frequency among a few adjacent modes: the intensity of each mode vanished regularly while keeping the sum of the intensities constant, thanks to an appropriate lag between alternating modes. Similar experimental results, though less clearly interpretable, had been obtained in "long-wavelength" lasers ($\lambda \approx 1.3$ μm) [12] and even more complex dynamics has since been observed in multimode quantum dot lasers [13]. The most striking point of these observations is the occurrence of a regular modal dynamics devoid of the amplitude modulation which was customarily associated with modal jumps [8,9].

Phenomenological modeling for this new dynamical regime was proposed by introducing mode coupling through nonlinear mechanisms [10,14] or through noise [15]. Subsequently, a model based on a Ginzburg-Landau equation proposed a more fundamental description [16] but its predictions have been shown to be nothing else but extremely long transients [17].

Here, thanks to a codimension 2 bifurcation analysis [18,19] of the fundamental equations governing multimode dynamics for a semiconductor laser near its threshold, we prove the existence of pure phase instability (characterized by a periodic oscillation of the optical frequency and a constant intensity) as well as of mixed phase-amplitude turbulence regimes. We thus provide a *fundamental*, alternative satisfactory interpretation of the deterministic multimode dynamics observed in some semiconductor lasers.

The main features of our model [3,20] can be summarized as follows. The electric field E, polarized along x and propagating along z, satisfies

$$\partial_{tt}E + \frac{1}{\epsilon_0}\partial_{tt}P = c^2\partial_{zz}E - \sigma\partial_t E, \tag{1}$$

where $P(t,z)$ is the dielectric polarization, ϵ_0 and c are the dielectric constant and the speed of light in vacuum, respectively, and σ represents losses. The carrier density obeys

$$\partial_t N = \gamma(N_p - N) + D\partial_{zz}N + \frac{2}{\hbar\omega_c}E\partial_t P, \tag{2}$$

where γ is the carrier's relaxation constant, N_p the pump parameter, D the diffusion constant, $\hbar$ Planck's constant, and ω_c is the oscillation frequency. The Fourier transforms of E and P are related through the susceptibility $\chi(\omega, N)$:

$$\widehat{P}(\omega) = \epsilon_0 \chi(\omega, N)\widehat{E}(\omega). \tag{3}$$

Close to transparency (obtained for $N_p = N_{pc}$), three independent slow characteristic time scales appear and are associated with (i) the electric field amplitude growth rate (related to the distance $\Delta N = N_p - N_{pc}$ from transparency), (ii) the population inversion time constant (γ^{-1}), and (iii) $\Gamma^{-1} \propto (\partial\chi/\partial\omega)|_{\omega_c, N_{pc}}$ which characterizes the susceptibility's frequency dependence near resonance.

Looking for a solution for Eq. (1) of the form $E = e^{\lambda t} e^{ikz}$ in the neighborhood of transparency (i.e., for small variations dN, $d\lambda$, and dk) and setting $N = N_{pc} + dN$, $\lambda = i\omega_c + d\lambda$, $k = k_c + dk$, we obtain

$$\frac{d\lambda}{\omega_c}\left[2i(1+\chi) + i\omega_c \frac{\partial\chi}{\partial\omega} + \frac{\sigma}{\omega_c}\right] = N_{pc}\frac{\partial\chi}{\partial N}\frac{dN}{N_{pc}} - 2\frac{c^2 k_c^2}{\omega_c^2}\frac{dk}{k_c}, \tag{4}$$

where we have dropped ω_c and N_{pc} from the functional dependence, thereby replacing $\chi(\omega_c, N_{pc})$, $(\partial\chi/\partial N)|_{\omega_c, N_{pc}}$, …, with χ, $\partial\chi/\partial N$, …. Then, taking into account the smallness of following experimentally determined parameters

$$\frac{\gamma}{\omega_c} \simeq 10^{-6}, \qquad \frac{\Gamma}{\omega_c} \simeq 10^{-3}\,\frac{Dk_c^2}{\omega_c} \simeq 10^{-3}, \qquad \frac{\sigma}{\omega_c} \simeq 10^{-3}, \tag{5}$$

we can rewrite

$$\frac{d\lambda}{\omega_c} \propto \left(\frac{\Gamma}{\omega_c}\right)\frac{dN}{N_{pc}}, \qquad \frac{dk}{k_c} \propto \frac{dN}{N_{pc}}. \tag{6}$$

The scaling law for the electric field amplitude can be estimated from Eq. (2) by neglecting the diffusion term for the population, considering equilibrium, and extracting a relation between N and E:

$$\gamma(N_p - N) \propto \frac{2}{\hbar\omega_c} E\partial_t P \Rightarrow E^2 \propto \frac{\hbar\omega_c N_{pc}}{\epsilon_0}\left(\frac{\gamma}{\sigma}\right)^{\frac{1}{2}}\left(\frac{dN}{N_{pc}}\right)^{\frac{1}{2}}. \tag{7}$$

While the usual procedures to reduce the dynamics take full advantage of the large separation between these time scales to perform the adiabatic elimination of the fast variables [21], here we adopt the diametrically opposite, but nevertheless well-established [18,19], point of view: upon approaching the laser transparency we seek to slow down the electric field envelope dynamics (controlled by dN/N_{pc}) until it becomes as slow as that of the population inversion (controlled by γ/ω_c). As usual for codimension 2 analysis, there is no rigorous, fully satisfactory way of choosing the exponent ($x > 0$) which measures the ratio between the two characteristic times $(dN/N_{pc}) = (\gamma/\omega_c)^x$. Several values of x are possible, each leading to a slightly different result. However, the terms appearing in the final envelope equations are always the same, the differences among expansions being limited to the rank in smallness parameter occupied by each term: physical relevance determines which terms ought to be retained. A full discussion of these technical details will be offered in a forthcoming publication [20], where we investigate the influence of x and compare several choices for its value. Here, as a good compromise between the accuracy and computing effort, we adopt $x = 1/2$.

The following scalings and definitions are now introduced:

$$\begin{aligned}
&\gamma = \omega_c\epsilon^2 \quad \text{definition of} \quad \epsilon,\\
&N_p = N_{pc}(1 + \tilde{\mu}\epsilon) \quad \text{with} \quad \tilde{\mu} \simeq \mathcal{O}(1),\\
&\sigma = \omega_c\epsilon\tilde{\sigma} \Rightarrow \chi_i = \frac{\sigma}{\omega_c} = \epsilon\tilde{\sigma},\\
&\Gamma = \omega_c\epsilon\tilde{\Gamma},\\
&D = \epsilon\frac{\omega_c}{k_c^2}\tilde{D},
\end{aligned} \tag{8}$$

with

$$\begin{aligned}
&N = N_{pc}(1 + \epsilon^1 S + \epsilon^2 N_2 + \cdots),\\
&E = \sqrt{\frac{\omega_c N_{pc}\hbar}{\epsilon_0}}(\epsilon^1 E_1 + \epsilon^2 E_2 + \cdots),\\
&P = \epsilon_0\sqrt{\frac{\omega_c N_{pc}\hbar}{\epsilon_0}}(\epsilon^1 P_1 + \epsilon^2 P_2 + \cdots),
\end{aligned} \tag{9}$$

and

$$\begin{aligned}
\partial_t &= \omega_c\left(\partial_{t_0} + \underbrace{\epsilon^2\partial_{t_2} + \epsilon^3\partial_{t_3} + \epsilon^4\partial_{t_4} + \cdots}_{\epsilon^2\partial_T}\right),\\
\partial_z &= k_c\left(\partial_{z_0} + \underbrace{\epsilon^1\partial_{z_1} + \epsilon^2\partial_{z_2} + \epsilon^3\partial_{z_3} + \cdots}_{\epsilon\partial_Z}\right).
\end{aligned} \tag{10}$$

We also introduce the dimensionless partial derivatives

$$\omega_c\frac{\partial\chi}{\partial\omega}\bigg|_{\omega_c, N} = \frac{\chi_\omega(N)}{\epsilon}, \qquad \omega_c^2\frac{\partial^2\chi}{\partial\omega^2}\bigg|_{\omega_c, N} = \frac{\chi_{\omega\omega}(N)}{\epsilon^2}, \tag{11}$$

so that $\chi_\omega(N)$ and $\chi_{\omega\omega}(N)$ are now of order 1.

The previous expansions are solutions of Eqs. (1), (2), and (3) up to $\mathcal{O}(\epsilon^3)$ provided that

$$\partial_T F = -V\partial_Z F + c_0 SF + \epsilon c_1\partial_{ZZ}F + \epsilon c_2 S\partial_Z F, \tag{12a}$$

$$\partial_T S = \tilde{\mu} - S - 4\tilde{\sigma}|F|^2, \tag{12b}$$

where

$$c_0 = \frac{N_{pc}\frac{\partial\chi_i}{\partial_N}}{\chi_\omega}(1-i\alpha), \qquad V = \frac{2c^2k_c^2}{\omega_c^2\chi_\omega},$$
$$c_1 = \frac{-V^2\chi_{i\omega\omega}}{2\chi_\omega}(1-i\beta), \qquad c_2 = \frac{-i\chi_{\omega\omega}Vc_0}{\chi_\omega} + \frac{N_{pc}V\frac{\partial\chi_\omega}{\partial N}}{\chi_\omega}, \tag{13}$$

with $\mathrm{Re}\{c_0\}$ and $\mathrm{Re}\{c_1\} > 0$ (by construction), $\alpha = (\partial\chi_r/\partial N)/(\partial\chi_i/\partial N)$ is the usual alpha factor and β a new, real function defined as

$$\beta = \frac{\chi_\omega}{V\chi_{i\omega\omega}}\left(\frac{\chi_{r\omega\omega}V}{\chi_\omega} - 1\right). \tag{14}$$

Eq. (12a) contains not only the usual slowly varying envelop terms for class B semiconductor lasers [22,23], but also additional smaller new terms. The term containing the complex coefficient c_1 represents diffusion (as in [16]) but also dispersion of the electric field, while the one containing c_2 describes group velocity and wave vector renormalizations associated with the distance from the threshold.

We examine the stability of the spatially homogeneous solution ($S = 0$, $F = \sqrt{\tilde{\mu}/4\tilde{\sigma}}$)—i.e., the monochromatic solution selected by the gain at the threshold—looking at its critical eigenvalue (λ_ϕ) associated with the time translation invariance symmetry. This eigenvalue can be shown to be expandable in power of k as

$$\lambda_\phi = [l_2k^2 + l_4k^4 + \mathcal{O}(k^6)] + i[-Vk + \mathcal{O}(k^5)], \tag{15}$$

with

$$l_2 = -\epsilon\frac{c_{0r}c_{1r} + c_{0i}c_{1i}}{c_{0r}}, \quad = -\epsilon c_{1r}(1+\alpha\beta),$$
$$l_4 = -\epsilon^2\frac{c_{1i}^2(c_{0r}^2 + c_{0i}^2)}{2c_{0r}^3\mu} \le 0. \tag{16}$$

We make the following remarks. (i) $l_4 < 0$, thus the small scales are damped. (ii) l_2 is the usual *Benjamin-Feir* phase instability control parameter [1]. $l_2 < 0$ corresponds to the stability of the single mode solution, while $l_2 > 0$ yields a phase-unstable regime with possible cyclic oscillations in the optical frequency (as observed in [10–13]). (iii) The crucial difference between Eq. (12) and those of [16] lies in the existence of c_{1i}. Indeed, if $c_{1i} = 0$ the leading term in $\mathrm{Re}\{\lambda_\phi\} < 0$ and the monochromatic solution remains stable, as in [16], although long transients ($\lambda_\phi \propto (\epsilon/L^2)$, L laser length) may be mistaken for multimode dynamics [17]. (iv) $l_2 > 0$ if $\beta < -1/\alpha < 0$; thus, the instability is controlled by (c_{1i}/c_{1r}) rather than $|c_1|$ (small). (v) When $l_2 < 0$, $\max\{\mathrm{Re}\{\lambda_\phi\}\}$ for $k_{\max}^2 \simeq -(l_2/2l_4)$, which, substituted into $\mathrm{Im}(\lambda_\phi)$, gives a periodic oscillation of the optical frequency at $\Omega \simeq Vk_{\max}$. Since l_2 can approach zero, there is no lower bound for the oscillation frequency Ω and the cyclic changes in laser frequency can be as slow as desired. This feature closely matches the experimental observations, since the frequencies with which the lasing modes cycle [10,11] are at least 3 orders of magnitude smaller than the inherent oscillation frequencies typical of semiconductor lasers. As such, this observation was one of the most striking characteristics of the experimental findings [10,11] and one which was most difficult to interpret physically.

In order to estimate realistic physical values for β, thereby assessing the possibilities for $l_2 > 0$, we consider the analytical approximation for the susceptibility in multiple-quantum-well lasers [24]

$$\chi(\omega,N) = -\chi_0\left[2\log\left(1-\frac{v}{u-i}\right) - \log\left(1-\frac{b}{u-i}\right)\right], \tag{17}$$

where χ_0 is constant, $v = (N/N_{pc})$, and $u = [(\omega - (E_t/\hbar))/\Gamma]$. Band-gap renormalization effects due to the screened Coulomb interaction between electrons and holes can be taken into account by renormalizing the transition energy E_t,

$$E_t(N) = \hbar\omega_c - aN^b \Rightarrow u = \frac{\omega-\omega_c}{\Gamma} + p_s\left(\frac{N}{N_{pc}}\right)^b, \tag{18}$$

where $p_s = (aN_{pc}^b/\hbar\Gamma)$ is the band-gap shrinkage parameter [24]. The coefficients a and b are material dependent and can be experimentally determined from [25,26]. In Fig. 1 we plot $(1+\alpha\beta)$ ($\propto l_2$) vs normalized losses $\tilde{\sigma}$ (equivalent to changing transparency N_{pc}). In the absence of band-gap renormalization $(1+\alpha\beta) > 0$; thus, $l_2 < 0$ for any reasonable value of normalized losses (solid line), while the band-gap renormalization (dashed and dash-dotted lines, cf. caption) may lead to a phase-unstable regime, thus proving that the phase instability is physically accessible and offering a viable interpretation for the experiments [10–13].

Other approximate properties of Eq. (12) may be inferred from the comparison with the complex Ginzburg Landau equation (CGLE), for which a vast literature exists [27].

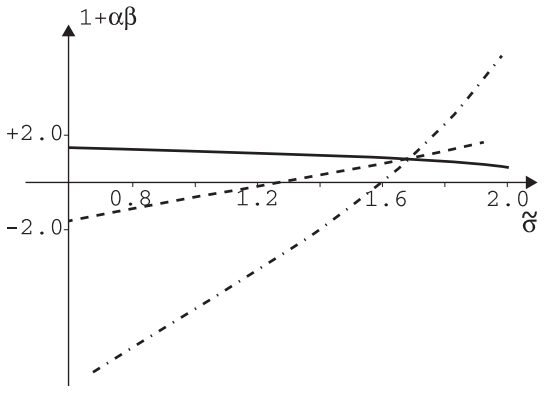

FIG. 1. Benjamin-Feir stability boundary vs $\tilde{\sigma}$. The susceptibility is taken as in [24], without (solid line) and with a band-gap renormalization estimated from the experimental measurements of [25] (dashed line) or [26] (dash-dotted line).

In the CGLE, the phase instability appears either as pure phase turbulence or as a mixture of phase and amplitude turbulence [28]. Although the phase gradients are strongly fluctuating in both cases, in the former the amplitude is almost constant, while in the latter its dynamics is also turbulent. For comparison with the CGLE, even though not entirely justifiable, we perform the standard adiabatic elimination of S (setting $S \simeq \tilde{\mu} - 4\tilde{\sigma}|F|^2$ and substituting into the electric field equation), obtaining

$$\partial_T F \simeq c_0\tilde{\mu}F - V\partial_Z F - 4\tilde{\sigma}c_0|F|^2F + \epsilon c_1\partial_{ZZ}F + \cdots. \tag{19}$$

By analogy, we then expect (i) a pure phase-unstable regime for small c_{0i}/c_{0r} and large c_{1i}/c_{1r}, and (ii) an amplitude turbulent regime for large c_{0i}/c_{0r} and small c_{1i}/c_{1r}. In the pure phase-unstable regime, where the amplitude dynamics is enslaved to that of the phase gradients, the adiabatic elimination of the amplitude leads to the well-known Kuramoto-Sivashinsky phase equation [27] for which the number of positive Lyapunov exponents is shown to linearly increase with the system's size [29]. Thus, we expect the phase instability to act as an *intrinsic noise generator* for the laser's electric field amplitude.

The numerical simulations of Eq. (12) are performed with a standard fourth order Runge-Kutta algorithm in time and a sixth order finite-difference method to approximate the spatial derivatives. Varying the space and time increments, we have carefully checked that numerical noise does not qualitatively affect our predictions. The simulations are performed, as usual, with periodic boundary conditions (unidirectional cavity), rather than with the Fabry-Perot configuration used in the experiments [10–13].

Given the long relaxation time scales expected from the phase dynamics, in order to ensure convergence in the simulations, we first explore the phase-stable regime. For the parameter values of Fig. 4(a), the slowest phase gradient decay rate is $\lambda_\phi(2\pi/L) \sim 3 \times 10^{-6}$. Thus, we expect, and do observe, that the initial phase gradients vanish after a characteristic time $\tau \sim 10^6$. On the basis of this result, in the following figures we only show predictions obtained in the asymptotic regime.

By analogy with the CGLE, we associate the numerical observations of Fig. 2 with an amplitude turbulence regime, where not only the phase gradients but also the amplitude strongly fluctuate in space and time. The associated power spectrum is shown in Fig. 4(d). This parameter regime should correspond to the experimental observations obtained far from threshold, where no particular modal sequence was observed and where the total intensity oscillates irregularly [30].

Figure 3 has been numerically obtained in the pure phase-unstable regime (small α, large β). The electric field frequency displays regular variations with asymmetric periodic cycling. Only a few modes are involved in the dynamics [Fig. 4(c)] and the total intensity is nearly constant. These predictions are in very good qualitative agreement with the experimental observations of deterministic mode switching [11], with a discrepancy in the intensity bandwidth: in the experiment the intermode beatings—if present—could not be detected, while in our calculations they are truly absent.

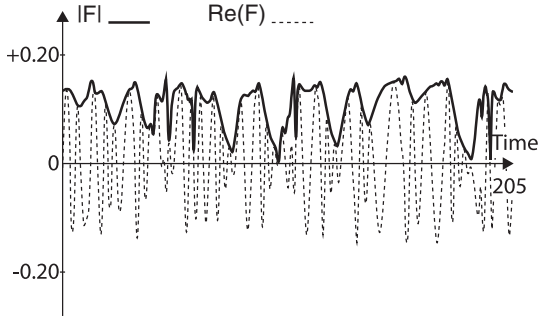

FIG. 2. Numerical simulation of Eq. (12) in the amplitude turbulence regime. Some parameters are common to all our simulations: $\mu = 0.1$, $\sigma = 2$, $D = 1$, $\chi_r = 3$. Specific to this simulation, the length L of the numerical box is 512, $c_0 = 0.0050 + i0.0065$, $c_1 = 0.25 - i0.225$, and $c_2 = -i2.5006$. The continuous line stands for the amplitude evolution with time, at a fixed spatial position, the dashed one for the real part of F versus time. The dynamics is clearly turbulent.

Finally, we have simulated Eq. (12) in a phase-stable regime but with the addition of white noise in space and time uniformly distributed between $\pm\zeta\sqrt{dt}$ where dt is the time increment and $\zeta = 4 \times 10^{-3}$. The aim is to compare the effect of externally injected noise to the action of the phase instability. Although the latter involves a much narrower frequency range, they both produce multimode dynamics with somewhat differing spectral features [Figs. 4(b) and 4(c)].

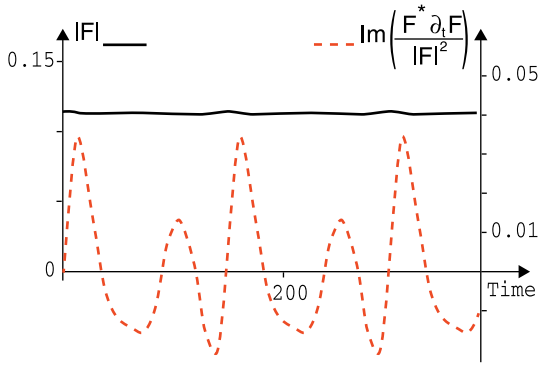

FIG. 3 (color online). Numerical simulation of Eq. (12) in the pure phase-unstable regime with $c_0 = 0.0125 + i0.0025$, $c_1 = 1.1955 - i11.9552$, and $c_2 = -i2.5006$. The length L of the numerical box is 119.3984. The top line (black online) represents the temporal evolution of the field amplitude, at a fixed spatial position, the bottom line (red online) the time derivative of the phase of F [i.e., $\mathrm{Im}[(F^*\partial_t F)/(|F|^2)]$]. As observed experimentally, the total intensity is constant and the electric field frequency oscillation is not symmetric.

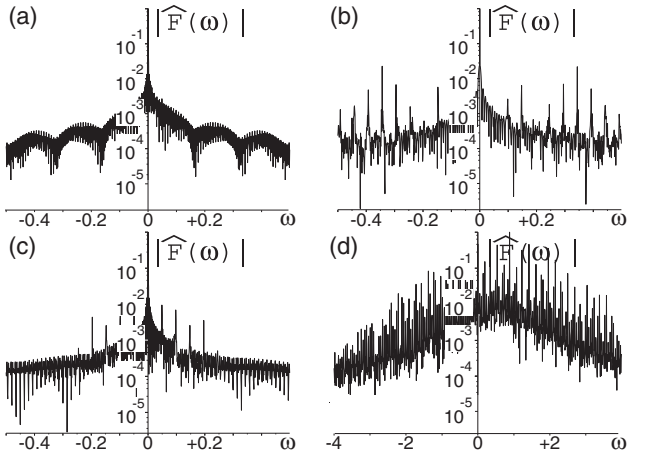

FIG. 4. Typical power spectra of F in log-linear scales obtained from the integration of Eq. (12). (a) Phase-stable regime with no added noise (aside from that of the numerical scheme): $c_0 = 0.01255 + i0.0025$, $c_1 = 1.1955$, $c_2 = 0$. (b) White noise added on space and time in the regime shown in (a). (c) and (d) Phase-unstable regime (no added noise)—(c) corresponds to the pure phase instability (cf. Fig. 3) and (d) to amplitude turbulence (cf. Fig. 2). The horizontal scale in panel (d) is approximately 10 times larger than that of the other three panels.

A physical interpretation for the meaning of the new β factor can be given by extracting the sign-changing parentheses in Eq. (14) and recasting it as $\beta \propto [(2c^2k_c^2/\omega_c^2)((\partial^2\chi_r)/(\partial\omega^2))/(\partial\chi/\partial\omega)^2 - 1]$, where we have explicitly written the derivatives, for clarity. For $\alpha > 0$, the common regime, a necessary (but not sufficient) condition for $\beta < 0$ is $(\partial^2\chi_r/\partial\omega^2) < (\omega_c^2/2c^2k_c^2)(\partial\chi/\partial\omega)^2$. Thus, the phase instability condition depends on the functional dependence of the refractive index with frequency, relating it to an anomalous dispersion regime or, analogously, to the self-focusing nonlinearity [31]. Since band-gap renormalization hardly affects β [20], a measurement of this parameter can be conducted (e.g., with ellipsometry or pump-probe experiments) practically at any injection level.

In conclusion, by computing the normal form description of a semiconductor laser bifurcation near its threshold, we have obtained a general model from which we deduce the existence of a new parameter β, proven, both analytically and numerically, to play a crucial role—in conjunction with the well-known α parameter—in the control of the phase instability. Our numerical simulations, predicting (asymmetric) periodic oscillations in the laser frequency as well as amplitude turbulent dynamics, are in good qualitative agreement with the experimental observations. Even though material-related and photon noise sources are always present, and can even be strong in semiconductor devices, our results show that in the phase-unstable regime these external noise components may only be an additional accessory which superposes some secondary randomness onto a regular or irregular, but still deterministic, behavior. Further work is needed to satisfactorily address this question.

We are grateful to two anonymous referees for constructing criticism which has allowed us to substantially improve this paper.

*lionel.gil@inln.cnrs.fr

[1] T. B. Benjamin and J. E. Feir, J. Fluid Mech. **27**, 417 (1967).
[2] G. P. Agrawal, *Nonlinear Fiber Optics*, 2nd ed. (Academic Press, San Diego, 1995).
[3] L. Gil and G. L. Lippi, Phys. Rev. A **83**, 043840 (2011).
[4] J. A. Copeland, J. Appl. Phys. **54**, 2813 (1983).
[5] C. H. Henry, P. S. Henry, and M. Lax, J. Lightwave Technol. **2**, 209 (1984).
[6] R. H. Wentworth, IEEE J. Quantum Electron. **26**, 426 (1990).
[7] R. Linke, B. Kasper, C. Burrus, I. Kaminow, J.-S. Ko, and T. Lee, J. Lightwave Technol. **3**, 706 (1985).
[8] M. Ohtsu and Y. Teramachi, IEEE J. Quantum Electron. **25**, 31 (1989).
[9] M. Ohtsu, Y. Teramachi, Y. Otsuka, and A. Osaki, IEEE J. Quantum Electron. **22**, 535 (1986).
[10] A. Yacomotti, L. Furfaro, X. Hachair, F. Pedaci, M. Giudici, J. Tredicce, J. Javaloyes, S. Balle, E. Viktorov, and P. Mandel, Phys. Rev. A **69**, 053816 (2004).
[11] L. Furfaro, F. Pedaci, M. Giudici, X. Hachair, J. Tredicce, and S. Balle, J. Quantum Electron. **40**, 1365 (2004).
[12] M. Yamada, W. Ishimori, H. Sakaguchi, and M. Ahmed, J. Quantum Electron. **39**, 1548 (2003).
[13] Y. Tanguy, J. Houlihan, G. Huyet, E. A. Viktorov, and P. Mandel, Phys. Rev. Lett. **96**, 053902 (2006).
[14] M. Ahmed, Physica (Amsterdam) **176D**, 212 (2003).
[15] M. Ahmed and M. Yamada, IEEE J. Quantum Electron. **38**, 682 (2002).
[16] C. Serrat and C. Masoller, Phys. Rev. A **73**, 043812 (2006).
[17] L. Gil and G. L. Lippi, Proc. SPIE Int. Soc. Opt. Eng. **9134**, 913413 (2014).
[18] G. Iooss and M. Adelmeyer, *Topics in Bifurcation Theory and Applications* (World Scientific, Singapore, 1998).
[19] M. Clerc, P. Coullet, and E. Tirapegui, Phys. Rev. Lett. **83**, 3820 (1999).
[20] L. Gil and G. L. Lippi (to be published).
[21] G. L. Oppo and A. Politi, Europhys. Lett. **1**, 549 (1986).
[22] L. Spinelli, G. Tissoni, M. Brambilla, F. Prati, and L. A. Lugiato, Phys. Rev. A **58**, 2542 (1998).
[23] L. Columbo, I. M. Perrini, T. Maggipinto, and M. Brambilla, New J. Phys. **8**, 312 (2006).
[24] S. Balle, Phys. Rev. A **57**, 1304 (1998).
[25] E. Lach, A. Forchel, D. Broido, T. Reinecke, G. Weimann, and W. Schlapp, Phys. Rev. B **42**, 5395 (1990).
[26] V. D. Kulakovskii, E. Lach, A. Forchel, and D. Grützmacher, Phys. Rev. B **40**, 8087 (1989).
[27] I. S. Aranson and L. Kramer, Rev. Mod. Phys. **74**, 99 (2002).
[28] H. Chaté, Nonlinearity **7**, 185 (1994).
[29] P. Manneville, in *Macroscopic Modelling of Turbulent Flows*, edited by U. Frisch, J. Keller, G. Papanicolau, and O. Pironneau, Lecture Notes in Physics, Vol. 230 (Springer, Berlin, 1985), pp. 319—326.
[30] X. Hachair (private communication).
[31] G. P. Agrawal, J. Opt. Soc. Am. **28**, A1 (2011).